



Distribution features and main controlling factors of volcanic buried hill reservoirs in carboniferous basement of Junggar Basin

Lin Zhou¹ · Kun Zhou² · Gang Wang³

Received: 15 July 2020 / Accepted: 28 November 2020 / Published online: 5 January 2021
© Saudi Society for Geosciences 2021

Abstract

On the northwestern margin of Junggar Basin, the complex volcanic oil reservoirs in the Carboniferous basement are highly concealed, poor physical properties, and difficult to explore or characterize. With the purpose of understanding the distribution of favorable reservoirs, the geological features, distribution law, and control factors of the reservoirs are fully explored based on analysis of the data from coring, logging, seismic analysis, and thin section in this paper. And some conclusions can be drawn as follows: (1) the Carboniferous rocks in the study area mainly include tuff lava, tuff, sedimentary tuff, tuffaceous sandstone, and tuffaceous glutenite; (2) the reservoirs have low porosity and permeability, the secondary pores and fractures provide the main storage spaces, the reservoirs fall into fractured reservoir and pored-fractured reservoir; (3) the favorable weathered crust reservoirs mainly exist in strong and moderately weathered zones in the vertical direction, which are 20–130 m from the top of the Carboniferous basement; in the planar direction, the reservoirs mostly concentrate around J353-J354-J336-J399-J132-J126 wells and around J12-J329 wells; (4) the reservoirs are mainly controlled by weathering and leaching, and the storage capacity is greatly improved by tectonic movement. This paper discloses the main controlling factors and distribution features of high-quality volcanic reservoirs in the Carboniferous basement on the northwestern margin of Junggar Basin, laying a solid basis and guidance for the exploration and development of similar oil and gas reservoirs.

Keywords Reservoir features · Distribution law · Main controlling factors · Volcanic rocks · Carboniferous basement

Introduction

The successful development of oil and gas reservoir in ancient buried hill of Renqiu Oilfield provides evidence to the exploration theory of ancient buried-hill reservoirs: the oil and gas generated in newer formations are stored in relatively older formations (Zhao et al. 2019; Li et al. 2006). Guided by this theory, China has managed to discover and develop various

types of buried-hill oil and gas reservoirs in many oilfields, namely, Liaohe Oilfield, Dagang Oilfield, and Shengli Oilfield (Fei and Wang 2005).

Based on lithology, the buried-hill oil and gas reservoirs can be divided into carbonate reservoirs, volcanic reservoirs, metamorphic reservoirs, and normal sandstone reservoirs. Many Chinese scholars have explored the reservoir features and controlling factors of ancient buried hills. However, the existing studies mainly focus on the paleo karstification and distribution law of carbonate reservoirs (Wang and Li 2017; Han et al. 2017). Despite being one of the four types of buried-hill reservoirs, volcanic reservoirs have not been studied on a global scale. The uniqueness of this type of reservoirs makes it difficult to be studied by a unified model or method.

The volcanic oil reservoirs in Junggar Basin are the most representative volcanic buried-hill reservoirs in China. These reservoirs are highly concealed, weakly porous, and difficult to explore or characterize (Wang et al. 2016; Chen et al. 2019; Tang et al. 2020). This paper mainly investigates the complex volcanic buried-hill reservoirs in Carboniferous basement of the basin. These reservoirs face multiple problems since

This article is part of the Topical Collection on *Big Data and Intelligent Computing Techniques in Geosciences*

✉ Lin Zhou
zhoulin285@126.com

¹ Exploration and Production Research Institute, SINOPEC Jiangnan Oilfield Company, Wuhan 430233, China

² Northeast Sichuan Gas Field, Petro China Southwest Oil & Gas Field Company, Dazhou 635000, China

³ Wugucheng Oil Production Crew, No. 9 Oil Production Plant, Changqing Oilfield, Yinchuan 750000, China

discovery: complex structures, strong heterogeneity, and unclear spatial distribution. Therefore, the author studied the volcanic reservoir in the study area from many aspects, in order to clarify the reservoir type, spatial distribution, and control factors and provide guidance for the later exploration and development.

The remainder of this paper is organized as follows: “Geological overview” summarizes the geology of the study area; “Basic features of reservoirs” identifies the basic geological features of Carboniferous volcanic reservoirs; “Distribution features of reservoirs” explores the distribution features of the reservoirs; “Influencing factors of reservoir distribution” discusses the main factors controlling the reservoir distribution; “Conclusions” puts forward the conclusions.

Geological overview

Located on the hanging wall of the Ke-Wu fault, the study area is next to Hongshanzui Oilfield in the southwest across the Ke-Wu fault and bordered in the west by the West Karamay Fault. The Carboniferous bedrock uplifted from the middle Carboniferous period to the end of the Jurassic

period, pushing away the Permian strata. The bedrock was weathered and then deposited, ending up in an unconformable contact with the overlying Triassic strata.

As shown in Fig. 1, the top of the Carboniferous basement appears as a monocline from the east to west. The dip angle of the monocline falls between 6° and 8° and increases to 25° near the Ke-Wu fault. The inside of the basement is extremely fractured. In the planar direction, the faults mostly spread in the south-north direction, and partly in the east-west direction; the planar distributions of the faults could be categorized into three patterns: parallel lines, oblique intersections, and broom shape. In the vertical direction, the faults exist in imbricated structure or as back-thrusts.

The major oil source of the study area is Mahu Sag. The oil and gas mostly migrate through the Ke-Wu fault, which is controlled by the overall tectonic setting of the northwestern margin of the Junggar Basin. The fault system in the study area at once blocks and facilitates the migration and accumulation of oil and gas. In the planar direction, the accumulation and reservoir-forming are controlled by fault blocks and fractures. In the vertical direction, the oil and gas reservoirs concentrate along the erosion surface of the Carboniferous basement, without any unified oil-bearing interface; the reservoirs vary greatly in height.

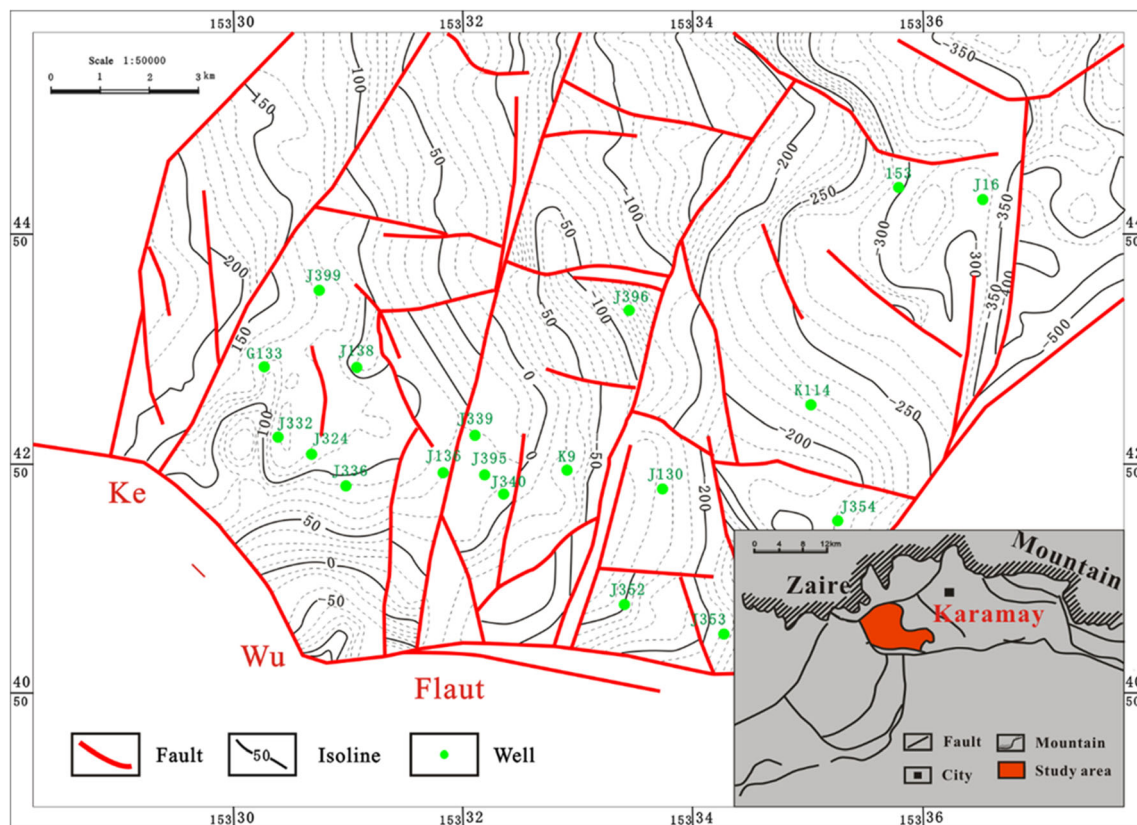


Fig. 1 The structure of the top of the Carboniferous basement

Basic features of reservoirs

Petrological features

In the study area, the Carboniferous basement of the volcanic buried-hill reservoirs mainly consists of volcanoclastic rocks. Based on their formation mechanism, volcanoclastic rocks can be divided into volcanoclastic rocks in transition to lava rocks, normal volcanoclastic rocks, and volcanoclastic rocks in transition to sedimentary rocks (Chukwua and Obiora 2018; Umazano and Melchor 2020).

According to the data of coring, logging, and thin-section microscopy, the volcanoclastic rocks in the Carboniferous basement in the study area belong to volcanoclastic rock in transition to lava rocks (Fig. 2a), most of which are normal volcanoclastic rocks and volcanoclastic rocks in transition to sedimentary rocks (Table 1).

The normal volcanoclastic rocks include welded volcanoclastic rocks and tuff rocks (Shcherbakov et al. 2018). The volcanoclastic rocks, which mainly contain tuff, are more common in the study area than the welded volcanoclastic rocks. Structurally speaking, the welded volcanoclastic rocks can be subdivided into vitric tuff, lithic tuff, and crystalline tuff. The vitric tuffs are distributed unevenly in varied shapes; most of them have been devitrified into chlorites (Fig. 2b). The lithic tuffs are mainly composed of andesite, basalt, and rhyolite (Fig. 2c). The crystalline tuffs mostly contain feldspar, with a small amount of amphibole, pyroxene (Fig. 2d)

There are three types of volcanoclastic rocks in transition to sedimentary rocks: sedimentary tuff, tuffaceous sandstone, and tuffaceous glutenite. Sedimentary tuff, as a type of sedimentary volcanoclastic rock, is mostly (> 65%) made up of volcanoclastic materials (Fig. 2e). Meanwhile, tuffaceous sandstone and tuffaceous glutenite are both volcanoclastic sedimentary rocks, containing fewer (< 40%) volcanoclastic materials (Fig. 2f). The volcanoclastic materials include andesite, tuff, rhyolite, felsite, feldspar, and quartz. Among them, the feldspar is mainly albite and plagioclase.

To sum up, the volcanic rocks in the study area mainly include tuff, sedimentary tuff, tuffaceous sandstone, and tuffaceous glutenite. Overall, tuff is the most widely developed type of rock in the study area. This type of rock dominates the top of the Carboniferous basement, supplemented by sedimentary tuff and tuffaceous sandstone. Tuff is mostly developed at the center of the study area, while volcanoclastic sedimentary rocks (i.e., sedimentary tuff and tuffaceous sandstone) are generally developed on the two wings of the study area.

Space features of reservoirs

Reservoir spaces are either primary or secondary (Kassab et al. 2016; Temraz and Dypvik 2018). Due to the influence of diagenetic compaction, most reservoir spaces are secondary in the volcanic buried-hill reservoirs (Ge et al. 2020; Li et al. 2019). According to the data of coring, fluorescence, and casting thin-section microscopy, pores and fractures coexist in the

Table 1 The classification and features of Carboniferous rocks in the study area

Classification	Subclass	Rock type	Feature
Volcanoclastic rocks in transition to lava rocks	Volcanic clastic lavas	Tuff lava	It is less distributed in the work area and only observed on a few drilling cores (for example, Andesite tuff lava in well 42937), which is mainly a kind of volcanoclastic lava formed by the volcanoclastic material falling into the molten slurry. The content of volcanoclastic material is between 30 and 50%
Normal volcanoclastic rocks	Welded volcanoclastic rocks	Lithic tuff	The detritus is mainly composed of andesite, basalt, and rhyolite, with a small amount of amphibole
		Crystalline tuff	It is less distributed in the work area, only in a small number of wells in the study area, with different crystal chip shapes
		Vitric tuff	The pyroclastic materials are mainly glassy debris with different shapes and uneven distribution, most of which have been devitrified and chloritized
Volcanoclastic rocks in transition to sedimentary rocks	Volcanoclastic rocks	Tuff	One of the main rock types in the study area, mainly composed of various rock cuttings, glass cuttings, crystal cuttings and volcanic ash, distributed in most of the wells in the study area
		Sedimentary tuff	The pyroclastic material accounts for more than 65%, and the particle size of the pyroclastic material is less than 2 mm. The clastic composition is andesite, tuff, rhyolite and felsite, feldspar, and quartz; feldspar is mainly albite and plagioclase
		Tuffaceous sandstone	The pyroclastic material is less than 40%, it is only distributed in some wells in the work area
	Volcanoclastic rocks	Tuffaceous glutenite	The pyroclastic material is less than 40%, less proportion in the study area.

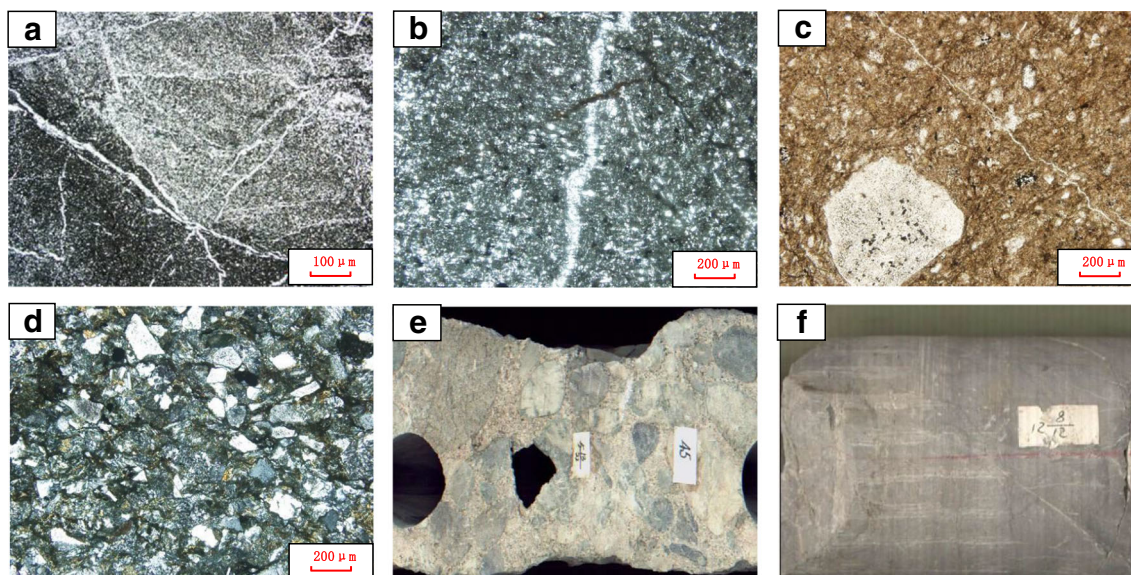


Fig. 2 The petrological features of Carboniferous volcanic rocks in the study area. **a** Tuff lava, well 42793; **b** welded volcanoclastic rocks, well 42793; **c** tuff rocks, well 43119; **d** tuff rocks well 43119; **e** tuffaceous conglomerate well K114; **f** tuffaceous sandstone, well 153

reservoir spaces of the Carboniferous volcanic reservoirs in the study area (Table 2). The pores include primary pores and secondary pores. The secondary pores and fractures of the Carboniferous reservoirs in the study area provide the main migration channels and storage spaces of oil and gas.

The primary pores mainly include inter-crystal pores (Fig. 3a), primary gas pores, intra-granular pores, intergranular pores, and residual pores. The secondary pores cover various dissolved pores, such as inter-crystal dissolved pores, dissolved holes and caves, etc. Specifically, inter-crystal dissolved pores are expanded from inter-crystal pores and inter-crystal micro-pores through dissolution. These pores are irregular in shape, with dissolved harbor-like edges. The pore size

and surface porosity of inter-crystal dissolved pores are 0.1–0.6 mm and 2–8%, respectively (Fig. 3b).

The dissolved holes and caves refer to the pores formed through the dissolution of gypsum clasts, gypsum particles, salt crystals, gravel-sized grains, sand-sized grains, and oolitic particle. The dissolved holes are 8 mm in size, while the dissolved caves are > 2 mm in size. The dissolved holes and caves are circular, ellipse, or irregular in shape and distributed in layers, beads, spots, or isolated islands. The pore size and surface porosity of the dissolved holes and caves are 0.03–2 mm and 1–8%, respectively. In some areas, the surface porosity is as high as 20–30% (Fig. 3c and d). The secondary pores are the combined results of epidiagenesis and the leaching of atmospheric water.

Table 2 The core fractures of Carboniferous volcanic rocks in the study area

Well	Core lengths (m)	Core number	Number of fractured cores	Fracture fillings	Remarks
42793	49.94	1	1	Calcite, small amount of pyrite	Development of mesh fracture, diagonal fracture, straight split fracture, horizontal fracture
42114	31.3	4	2	Calcite	Development of mesh fracture pyrite seen in rocks
42136	10.35	1	1	Calcite	Development of mesh fracture diagonal fracture
42785	49	3	3	Calcite, small amount of quartz and pyrite	Development of diagonal fracture straight split fracture
J354	77.1	5	2	Calcite, talc, chlorite	The top of the core are rich in pyrite without fracture
42757	20.26	7	7	Calcite, small amount of feldspar and pyrite	Development of straight split fracture microfracture
43119	47.66	1	1	Calcite, oil	Development of microfracture, diagonal fracture, straight split fracture
43110	47.54	1	1	Calcite, oil	Development of microfracture, mesh fracture, diagonal fracture, straight split fracture

Fractures serve as important storage spaces and seepage channels for oil and gas in volcanic reservoirs (Gilmer et al. 2017). Through the comprehensive analysis of outcrop survey, core observation description, and logging interpretation, it is found that the fractures in the study area include weathering fractures, tectonic fractures, tectonic dissolution fractures, and shrinkage fractures (Table 2).

Weathering fractures are formed through the weathering and leaching of rocks. These fractures spread in random directions. Each fracture is small yet wide and 5–20 cm in length. The weathering fractures are often filled with calcite and columnar anhydrite vertically to the fracture wall (Fig. 3e).

Tectonic fractures are distributed in various types of rocks. These fractures often run in parallel groups, pointing to the same direction. Different groups crisscross each other. Tectonic fractures cut through crystals or volcanoclastic particles, connecting pores along the path (Fig. 3f).

Tectonic dissolution fractures are generated under the combined effects of tectonic movement and weathering. In other words, tectonic dissolution fractures are essentially weathered

tectonic fractures. With irregular walls and large widths, these fractures are usually filled with freshwater calcite (Fig. 3g).

Shrinkage fractures are produced as magma is ejected to the surface and the magmatic rocks shrink due to the sharp temperature drop. These fractures are rarely seen on the cores, because the shrinkage fractures in volcanic rocks are weathered (Fig. 3h).

A large number of micro-fractures are observable in the cast thin sections. These micro-fractures differ in formation mechanism and extend across a small distance (Fig. 3i).

In general, most of the Carboniferous cores in the study area are fractured. The coring data show that the fractures have good oil-bearing properties and various filling materials: crude oil calcite, talc, chlorite, pyrite, and quartz. The diversity of filling materials indicates that the fractures in the Carboniferous basement are formed in different periods.

In terms of shape, the fractures can be divided into straight split fractures, micro-fractures, diagonal fractures, horizontal fractures, and mesh fractures. Mesh fractures are common across the Carboniferous basement. In the study area, the Carboniferous cracks are featured by small extension, high density, and obvious width change.

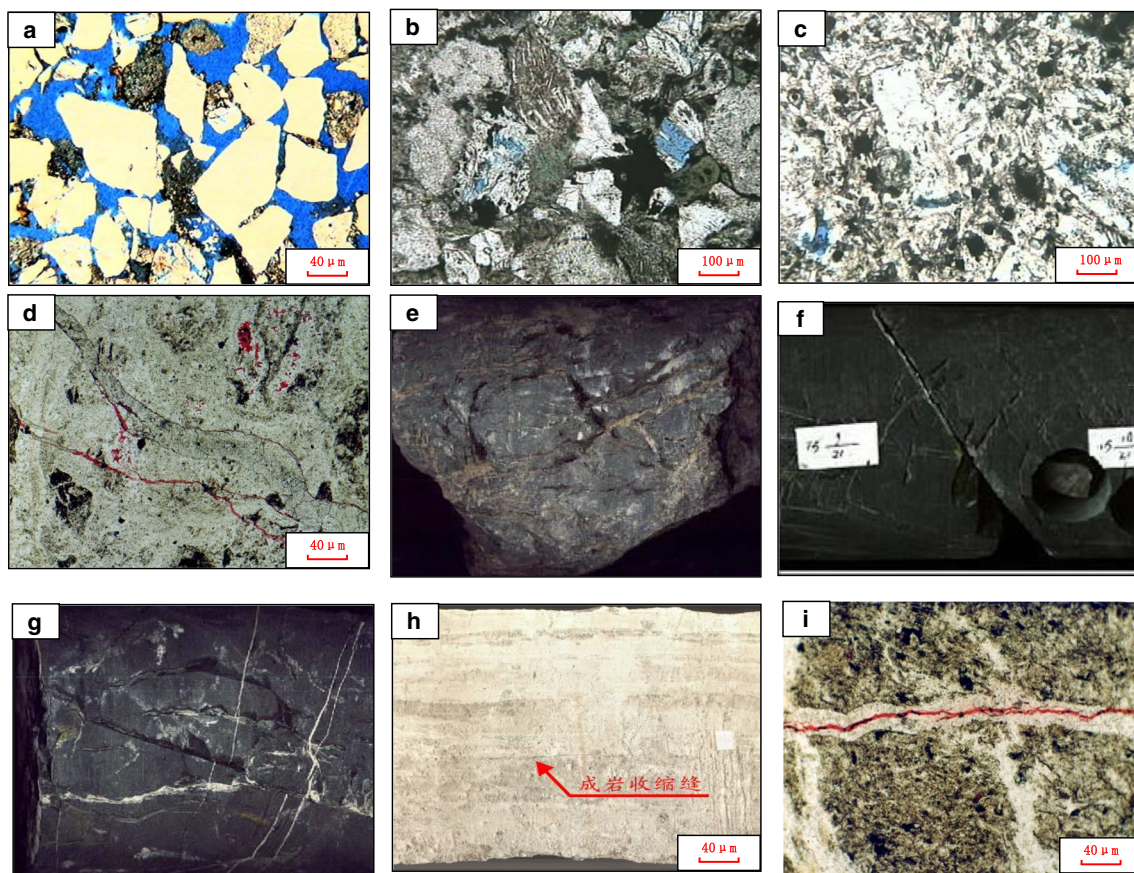


Fig. 3 The types of reservoir spaces in Carboniferous volcanic rocks of the study area. **a** Intergranular pore, well 43119; **b** almond dissolved pore, zeolite filling, well J15; **c** intragranular and intercrystalline dissolved pore, well J15; **d** dissolution fracture, well 42793; **e** weathering

fracture, well K114; **f** structural fracture, well 42793; **g** structural weathering fracture, well K114; **h** diagenetic fracture, well 45193; **i** micro fracture, well 43119

Physical features of reservoirs

In the study area, the Carboniferous volcanic rocks are extremely dense and hard, and the matrix is only slightly porous and permeable. Through the statistical analysis of the physical property test data of more than 260 samples, the porosity falls in 0.1–8%, averaging at 1.3%; the permeability falls in $(0.001\text{--}27) \times 10^{-3} \mu\text{m}^2$, averaging at $0.035 \times 10^{-3} \mu\text{m}^2$.

In terms of capillary pressure, the pores in the matrix are relatively poor, with small mercury saturation and mean size of $13.5\phi\text{--}13.7\phi$. Under the capillary radius, the pores are basically disconnected, making little contribution to oil and gas migration and storage.

The reservoir spaces are highly fractured, which greatly improves the seepage conditions of Carboniferous reservoirs. The Carboniferous reservoirs fall into two models: fractured reservoir and pored-fractured reservoir, the former is the main reservoir type. In fractured reservoirs (Fig. 4a), the fractures, mostly mesh fractures, are interconnected; slight dissolution takes place along the fractures; the matrix has an extremely low porosity. In pored-fractured reservoirs (Fig. 4b), the fractures are indirectly connected; strong dissolution takes place along the fractures; the matrix pores are connected with the fractures. Relatively speaking, the physical properties of fractured porous reservoir are better than that of fractured reservoir

Distribution features of reservoirs

Vertical development law of reservoirs

In the study area, fractures serve as the main storage space of Carboniferous reservoirs. The vertical distribution of fractures reflects the distribution law of reservoirs in the vertical direction. The presence of fractures may induce changes to the physical properties of rocks, which could be seen on logging

curves. Hence, the fractures could be identified based on the features of logging curves (Jeanne et al. 2016).

Sorting out the data of 25 wells in the study area, the authors set up a fracture identification template, after the imaging logging of some wells. Then, a continuous well profile was established based on single-well interpretations. It can be seen that the fractures are poorly developed within 20 m from the top of the Carboniferous basement. Most fractures are developed between 20 and 130 m from the top of the basement. And the depth of fracture development in each well is different, indicating that the fractures are developed in a heterogeneous manner.

Due to the compaction and filling of the sediments, the pores and fissures are filled up within 20 m from the top of the Carboniferous basement, reducing the storage capacity of the rocks. As the depth increases, the early pores and fissures are less compacted or filled outside 20 m from the top of the basement. Thus, the rocks at this depth have a good storage capacity, forming a favorable reservoir zone. Dissolved pores are not formed at more than 130 m from the top of the basement: the rocks at this depth are beyond the ancient weathering crust, and thus not greatly affected by early weathering and leaching. Tectonic fractures are the only type of primary reservoir space at this depth.

According to the features, formation mechanism, and distribution law of reservoirs in the ancient weathering crust, the strata beneath the Carboniferous weathered crust in the study area were classified from the top to bottom into five weathered zones: completely weathered zone, strongly weathered zone, moderately weathered zone, weakly weathered zone, and non-weathered zone (Fig. 5).

The fully weathered zone lies within 20–30 m from the top of the Carboniferous basement. Under strong compaction and cementation, the weathering fractures are filled up by the overlying sediments. Thus, the fully weathered zone has basically no storage capacity.

The strongly and moderately weathered zones are between 20 and 150 m from the top of the Carboniferous basement. The

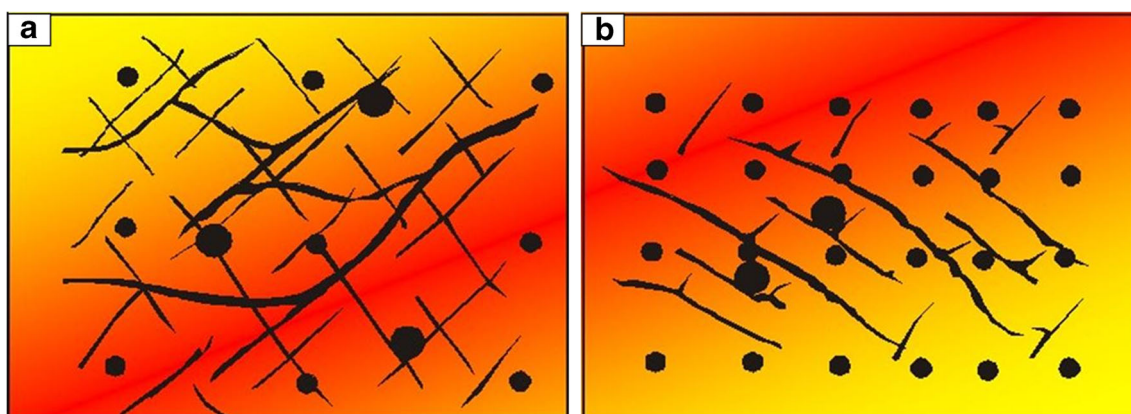


Fig. 4 The models of Carboniferous volcanic reservoirs in the study area. **a** Fractured reservoir. **b** Pored-fractured reservoir

strongly weathered zone has a pored-fractured reservoir space. This zone is severely fractured under weathering effect. There are numerous irregular mesh micro-fractures in this zone. The small fractures are mostly filled up. The storage capacity of this zone is modified by weathering, dissolution, and tectonic movement and damaged by compaction and cementation. The moderately weathered zone has a pored-fractured reservoir space. The rocks in this zone are fractured. The numerous large fractures link up pores.

The weakly weathered zone is not greatly affected by weathering and dissolution. With weakly fractured rocks, this zone has a certain storage capacity, thanks to the late tectonic movement. Tectonic fractures constitute the main reservoir space in this zone.

The non-weathered zone is over 300 m from the top of the Carboniferous basement. The storage capacity is extremely poor in this zone.

In the vertical direction, the volcanic reservoirs in the Carboniferous basement of the study area have poor storage capacity in the upper completely weathered zone and the bottom non-weathered zone. The favorable reservoirs mainly exist in strong and moderately weathered zones, which are 20–130 m from the top of the Carboniferous basement.

Planar distribution of reservoirs

According to coring, logging, and seismic data from the study area, the volcanic buried-hill reservoirs in the Carboniferous

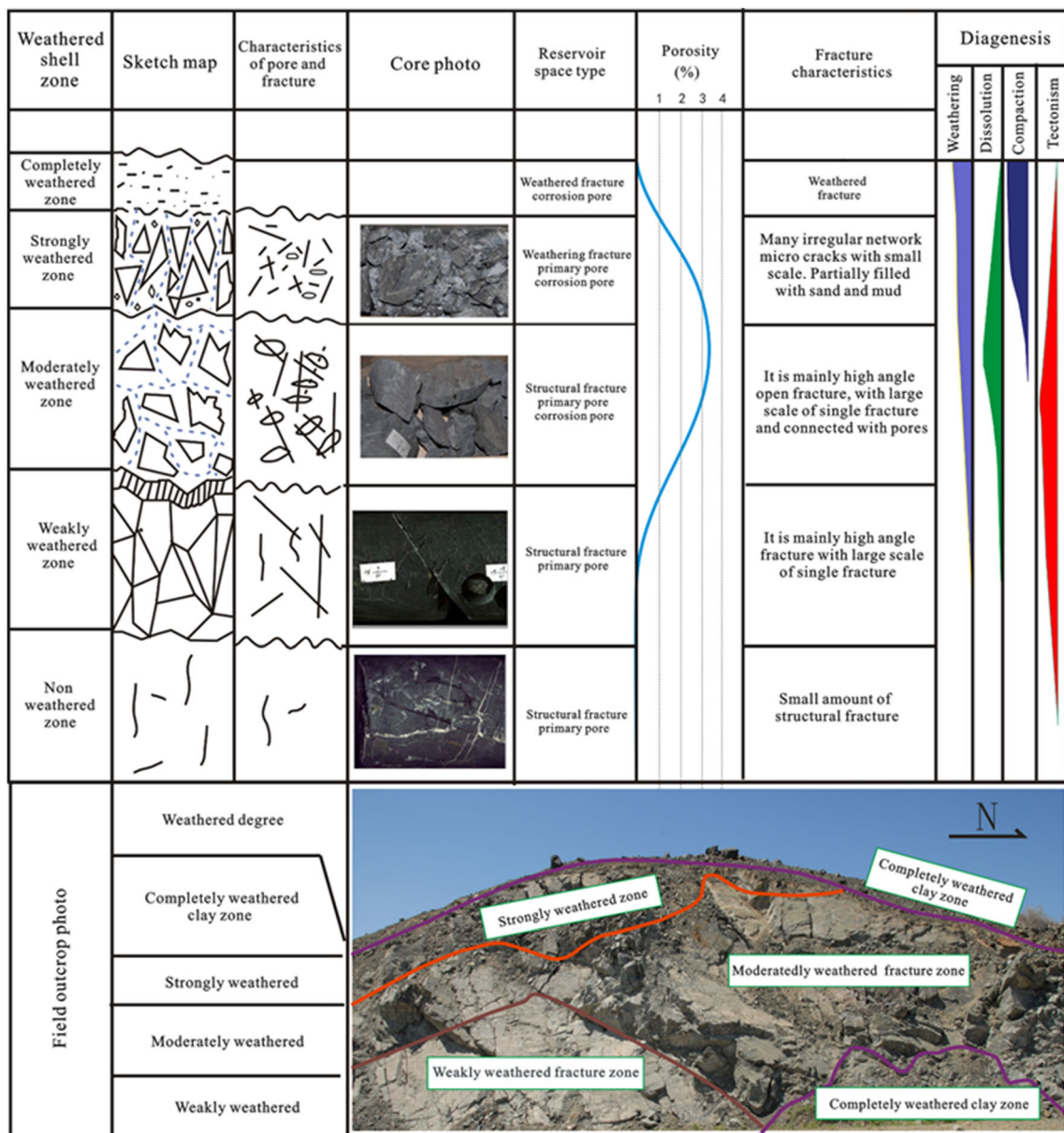


Fig. 5 The vertical development of Carboniferous reservoirs in the study area

basement were predicted to have two concentrated development zones in the planar direction (Fig. 6). The first zone is around J353-J354-J336-J399-J132-J126 wells. In this large zone, the reservoir thickness varies greatly. The blocks with reservoirs thicker than 100 m are sporadically distributed. The thickest reservoir appears near J125 well (> 150 m). The second zone is around J12-J329 wells in the northeast of the study area. The reservoirs in this zone are relatively thin, and similar in thickness.

In the planar direction, the Carboniferous volcanic reservoirs in the study area, controlled by the Ke-Wu fault, extend from southeast to the northwest and fall into several zones. The reservoirs are better developed at the center of the study area than in the peripherals.

Influencing factors of reservoir distribution

There are many factors that control the planar and vertical distributions of volcanic buried-hill reservoirs in the Carboniferous basement of the study area. In the planar direction, the reservoir distribution depends on the ancient weathered landform; in the vertical direction, the reservoirs are controlled by weathering and tectonic movement; in the meantime, the storage capacity of volcanic rocks is closely related

to the type of reservoir rocks (Lamur et al. 2017; Blusztajn et al. 2017).

Influence of the lithology and lithofacies of volcanic rocks

The quality of weathered crust reservoirs hinges on the type of volcanic rocks (Taheri et al. 2017). In the study area, the volcanic rocks are mainly tuffs, which are highly resistant to weathering. Despite the high intensity and long duration of weathering, the volcanic rocks are not severely weathered. The main weathering products are weathering fractures. The matrix pores are relatively undeveloped.

According to coring, logging, and seismic data from the study area, the Carboniferous strata belong to mid-basic central eruptive facies and crater facies. The lithofacies can be subdivided into near crater facies, hot debris flow subfacies, and heated base wave subfacies. The hot debris flow subfacies, under the eruptive facies, are widely distributed on the wing of the volcanic cone. The hot debris is condensed and deposited. Meanwhile, various reservoir spaces are developed, namely, inter-crystal pores, intergranular pores, and gas pores, resulting in good connectivity and physical properties. The reservoir spaces are later weathered, buried, and compacted, suppressing the storage capacity in a certain depth

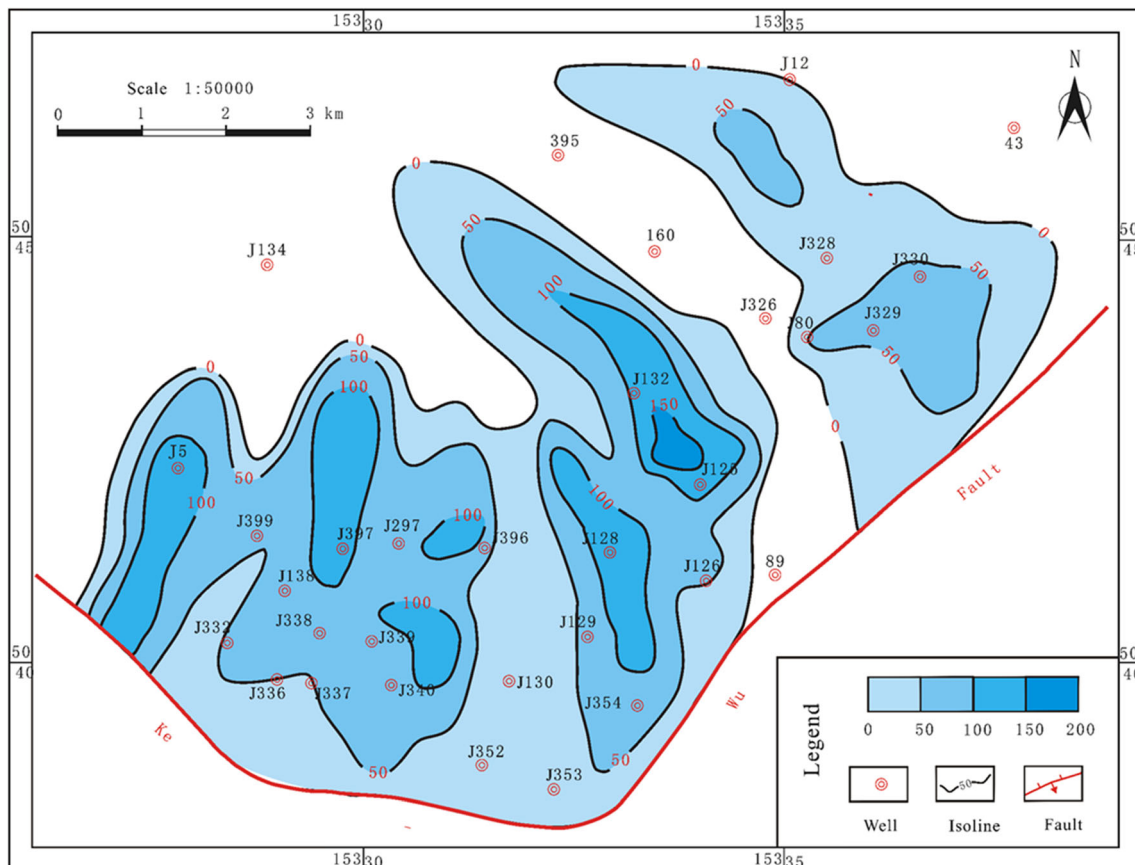


Fig. 6 The planar distribution of volcanic buried-hill reservoirs in the Carboniferous basement of the study area

below the top of the Carboniferous basement. But the belt of hot debris flow subfacies is generally a development zone of reservoir lithofacies.

Influence of weathering and leaching

For buried-hill reservoirs in Carboniferous basement, the reservoirs are directly controlled by the thickness of the weathered crust (Nakano et al. 2017; Wang and Wang 2016), which depends on the intensity of weathering and leaching. In the vertical direction, the weathering and leaching effects gradually weaken from the top to the bottom of the ancient weathering crust, causing a gradual decline in the quality of secondary reservoir spaces.

Note that the middle part of the ancient weathering crust has better storage capacity than the upper and lower parts, due to the later compaction and filling. Specifically, the secondary reservoir spaces are mostly compacted and filled up by the later sediments, within a certain distance from the top of the weathered crust; thus, the upper part has a limited storage capacity. The compaction and filling weaken outside that distance, such that most secondary fractures and pores can serve as effective reservoir spaces. The rocks have poor storage capacity at deeper levels, as the effects of weathering and leaching dwindle (Spotl et al. 1993).

Then, the distances from the top of the Carboniferous basement and physical properties of reservoirs were summarized and analyzed (Fig. 7). The results show that the physical properties of the reservoirs cyclically decrease with the distance from the top of the Carboniferous basement. The reservoir rocks have the best storage capacity within 200 m from the top of the Carboniferous weathered crust. Once the distance surpassed 300 m, the weathering and leaching effects become weak, leading to undeveloped fractures and dense rocks; the storage capacity is thus decreased. The reservoirs are basically undeveloped, at 400 m or more beneath the top of the weathered crust.

Combined with the previous analysis on reservoir distribution, the Carboniferous reservoirs in the study area are mainly controlled by weathering and leaching, followed by tectonic movement, in the vertical direction. The majority of reservoirs are distributed in 30–130 m below the top of the Carboniferous basement.

Influence of tectonic movement

The effect of tectonic movement on volcanic reservoirs is mainly reflected in fracture reconstruction (Bars et al. 2018; Garibaldi et al. 2020). After the nappe structure is formed in the northwestern margin, the rocks are reconstructed by tectonic movement. On the top of the Carboniferous basement, the rocks become highly plastic through the early weathering, leaching, filling, and compaction. The later tectonic movement only gives birth to a few amounts of fractures, which mainly connects the originally isolated pores. The fractures extend in random directions as a mesh. By contrast, tectonic movement can induce tectonic fractures in the lower rocks of the Carboniferous basement, which are less plastic due to the limited effects of weathering and leaching.

The segmented statistics on core fractures (Fig. 8) show that most fractures within 150 m from the top of the Carboniferous basement are weathering fractures (tectonic dissolution fractures are also counted as weathering fractures), which proportion are more than 50%. The proportion of tectonic fractures range from 20 to 40%, and shrinkage fractures are generally less than 10%. However, when the distance surpasses 150 m, there are more tectonic fractures than weathering fractures, indicating that the reservoirs deeper than 150 m are mainly controlled by tectonic movement. In summary, the fractures induced by tectonic movement exert two impacts on reservoirs: connecting the isolated pores and increasing the thickness of effective reservoirs in the vertical direction.

Fig. 7 The relationship between physical properties and distance from the top of Carboniferous basement of reservoirs

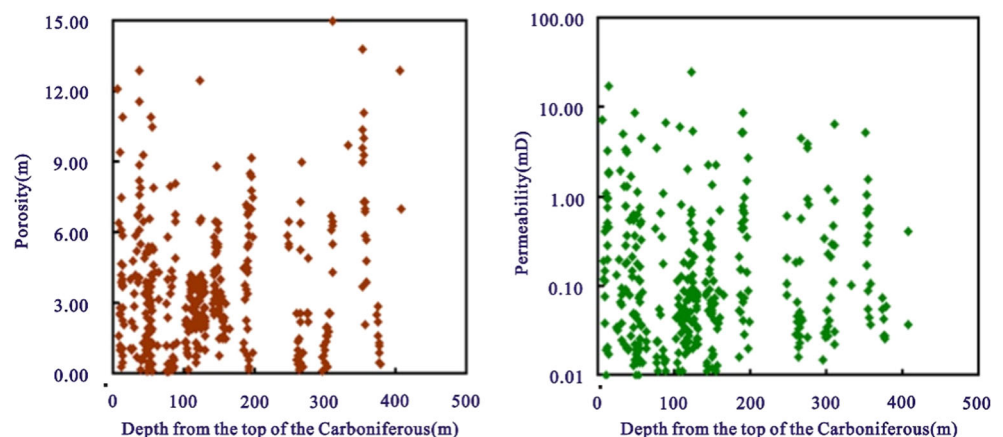
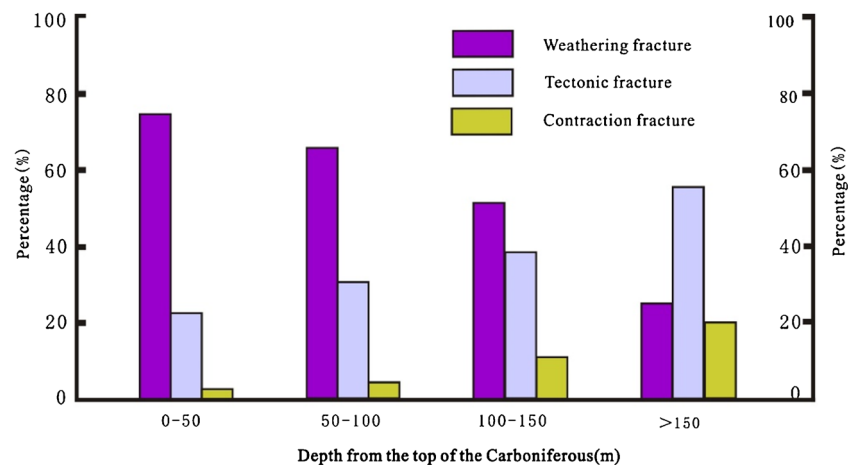


Fig. 8 The segmented statistics of fracture types in the Carboniferous cores from the study area



Conclusions

- (1) In the study area, most of the Carboniferous rocks are normal volcanoclastic rocks and volcanoclastic rocks in transition to sedimentary rocks, with a few amounts of volcanoclastic rocks in transition to lava rocks.
- (2) The matrix of Carboniferous reservoirs has extremely low porosity and permeability, and the secondary pores and fractures of the Carboniferous reservoirs in the study area provide the main migration channels and storage spaces of oil and gas.
- (3) In the vertical direction, the favorable reservoirs mainly exist in strong and moderately weathered zones, which are 20–130 m from the top of the Carboniferous basement. In the planar direction, the Carboniferous reservoirs in the study area mostly concentrate around J353-J354-J336-J399-J132-J126 wells and around J12-J329 wells.
- (4) The storage capacity of Carboniferous reservoirs is controlled by lithology and lithofacies, weathering and leaching, and tectonic movement.

References

- Bars A, Miao L, Fochin Z (2018) Petrogenesis and tectonic implication of the Late Mesozoic volcanic rocks in East Mongolia. *Geol J* 1:1–22
- Blusztajn J, Nielsen SG, Marschall HR (2017) Thallium isotope systematics in volcanic rocks from St. Helena—constraints on the origin of the HIMU reservoir. *Chem Geol* 476:292–301
- Chen SR, Qu XY, Qiu LW (2019) A statistical method for lithic content based on core measurement, image analysis and microscopic statistics in sand-conglomerate reservoir. *Instrum Mesure Métrologie* 18(4):343–352
- Chukwua A, Obiora SC (2018) Geochemical constraints on the petrogenesis of the pyroclastic rocks in Abakaliki basin (Lower Benue Rift), Southeastern Nigeria. *J Afr Earth Sci* 141:207–220
- Fei BS, Wang JH (2005) Cases of discovery and exploration of marine fields in China (Part 3): Renqiu Buried-hill Oilfield, Bohaiwan Basin. *Marin Orig Petr Geol* 10(3):43–50
- Garibaldi N, Tikoff B, Peterson D (2020) Statistical separation of tectonic and inflation-driven components of deformation on silicic reservoirs, Laguna del Maule volcanic field, Chile. *J Volcanol Geotherm Res* 389(1):1–13
- Ge LZ, Tong KJ, Meng ZQ (2020) Construction of an efficient development mode for buried-hill fractured reservoirs in Bohai Bay. *Adv Geo-energy Res* 4(2):162–172
- Gilmer AK, Sparks RSJ, Rust AC (2017) Geology of the Don Manuel igneous complex, central Chile: implications for igneous processes in porphyry copper systems. *Geol Soc Am Bull* 129(7-8):920–946
- Han Q, Yang ZC, Li HY (2017) Characteristics of Sandaoqiao buried hill structure and reservoir in the Northern Shaya uplift of Tarim Basin, China. *J Earth Sci Environ* 1:103–113
- Jeanne V, Albert G, Jean S (2016) Pre- and post-stimulation characterization of geothermal well GRT-1, Rittershoffen, France: insights from acoustic image logs of hard fractured rock. *Geophys J Int* 206(2):845–860
- Kassab MA, Abdou AA, Gendy NH (2016) Reservoir characteristics of some Cretaceous sandstones, North Western Desert, Egypt. *Egypt J Pet* 26(2):391–403
- Lamur A, Kendrick JE, Eggertsson GH (2017) The permeability of fractured rocks in pressurised volcanic and geothermal systems. *Sci Rep* 7(1):1–9
- Li J, Liu LF, Zhao YH (2006) A review of study on ancient buried hill reservoir. *Prog Geophys (in Chinese with English abstract)* 21(3):879–887
- Li J, Chen GP, Zhang B (2019) Structure and fracture-cavity identification of epimetamorphic volcanic-sedimentary rock basement reservoir: a case study from central Hailar Basin, China. *Arab J Geosci* 12(2):152–163
- Nakano N, Osanai Y, Nam NV (2017) Bauxite to eclogite: evidence for late Permian supracontinental subduction at the Red River shear zone, northern Vietnam. *Lithos* 302-303:37–49
- Shcherbakov VD, Nekrylov NA, Savostin GG (2018) The composition of melt inclusions in minerals from Tephra of the soil-pyroclastic cover of Simushir Island (Central Kuril Islands). *Mosc Univ Geol Bull* 73:31–42
- Spotl C, Matter A, Brevart O (1993) Diagenesis and pore water evolution in the Keuper Reservoir, Paris Basin (France). *J Sediment Res* 63(5):909–928
- Taheri M, Ardalan AA, Emami MH (2017) Petrology and tectonic setting of volcanic rocks in west and south west of Salafchegan, Qom, Iran. *Open J Geol* 7(6):745–767

- Tang Y, Zhai QG, Hu PY (2020) Southward subduction of the Bangong-Nujiang Tethys Ocean: insights from ca. 161–129Ma arc volcanic rocks in the north of Lhasa terrane, Tibet. *Int J Earth Sci* 109(2):631–647
- Temraz M, Dypvik H (2018) The Lower Miocene Nukhul Formation (Gulf of Suez, Egypt): microfacies and reservoir characteristics. *J Pet Explor Prod Technol* 8:85–98
- Umazano AM, Melchor RN (2020) Volcaniclastic sedimentation influenced by logjam breakups? An example from the Blanco River, Chile. *J S Am Earth Sci* 98:102477
- Wang YS, Li JY (2017) Characteristics and main controlling factors of layered reservoir in buried hill of carbonate rock in Pingfangwang Oilfield, Jiyang Depression. *J China Univ Petrl* 41(4):27–35
- Wang JM, Wang JJ (2016) The karst effect on the palaeokarst geomorphology and palaeokarst reservoir: a case study of the Ordovician weathering crust, eastern Ordos Basin, China. *Nat Gas Geosci* 27(8): 1388–1398
- Wang PJ, Jiao YY, Yang KK (2016) Classification of volcanogenic successions and its application to volcanic reservoir exploration in the Junggar basin, NW China. *J Jilin Univ* 46(4):1056–1070
- Zhao XL, Yang XB, Chen L (2019) Hydrocarbon accumulation conditions and exploration potential of carbonate buried hills in Weixinan sag in western South China Sea. *China Offshore Oil Gas* 31(2):51–61